International Atomic Energy Agency

INDC(CCP)-364
Distr.: G

INDC INTERNATIONAL NUCLEAR DATA COMMITTEE

SELECTED PAPERS ON NUCLEAR DATA ANALYSIS

(Translation of Russian Papers published in Yadernye Konstanty 1/1989)

Translation editor: Dr. A. Lorenz

February 1994

IAEA NUCLEAR DATA SECTION, WAGRAMERSTRASSE 5, A-1400 VIENNA

Reproduced by the IAEA in Austria
February 1994

INDC(CCP)-364
Distr.: G

SELECTED PAPERS ON NUCLEAR DATA ANALYSIS

(Translation of Russian Papers published in Yadernye Konstanty 1/1989)

Contents

Translation editor: Dr. A. Lorenz

February 1994

AVERAGE CROSS-SECTIONS USING R-MATRIX THEORY

A.A. Lukyanov, A.G. Vysotskij, N.B. Yaneva[*]

ABSTRACT

We present an analytical method for resonance cross-section averaging. A general formula for averaging the capture cross-section is derived exactly in the framework of the R-matrix formalism and using our resonance cross-section statistical model.

The description of average resonance cross-sections for neutron reactions is normally carried out using the Hauser-Feschbach formalism with corrections for the effect of resonance parameter fluctuations [1, 2]. This entails the use of certain approximations based on either a single-level description of resonance cross-sections in an averaging interval or on the assumption of a large number of reaction channels [2, 3]. In this paper, using our previously-proposed simplified model for multi-level description of cross-section energy structure taking into account resonance interference [2, 4], we propose an analytical method for cross-section averaging which is not dependent on the ratio between average widths and the spacings between levels.

Resonance cross-section model

We take as our starting point the expression for the diagonal collision matrix element in the framework of the R-matrix formalism [1]:

$$S_{nn}(E) = e^{-2i\varphi}[(1-iR)^{-1}(1+iR)]_{nn}, \qquad (1)$$

[*] Nuclear Research Institute of the People's Republic of Bulgaria, Sofia.

where φ is the potential scattering phase, and R is the matrix with elements

$$R_{nc}(E) = \frac{1}{2} \sum_{\lambda} \Gamma_{\lambda n}^{1/2} \Gamma_{\lambda n}^{1/2} / (E_\lambda - E - i\Gamma_\gamma/2), \qquad [2]$$

Here the radiation channels are taken into account by a corresponding imaginary addition to energy $i\Gamma_\gamma/2$ [1, 2]. We shall confine ourselves here to an example of single-channel elastic scattering with competing radiation capture. Then instead of matrix (2) we have the function

$$R = \frac{1}{2} \sum_{\lambda} \Gamma_{\lambda n} / (E_\lambda - E - i\Gamma_\gamma/2) = s \sum_{\lambda} x_\lambda / (\varepsilon + \pi\lambda + \delta_\lambda - iy), \qquad [3]$$

where:

$$s = \pi\bar{\Gamma}_n/2D, \; y = \pi\Gamma_\gamma/2D, \; \varepsilon = \pi(E_0 - E)/D, \; x_\lambda = \Gamma_{\lambda n}/\bar{\Gamma}_n, \; \delta_\lambda = \pi(E_\lambda - E - \lambda D))/D.$$

and D is the average resonance spacing. The corresponding scattering function

$$S = e^{-2i\varphi} \left(\frac{2}{1 - iR} - 1 \right) \qquad [4]$$

determines the energy dependence of the cross-sections, both total

$$\sigma(E) = 2[1 - Re\, S(E)] = 4[\cos^2\varphi - Re\, e^{-2i\varphi}(1 - iR)^{-1}], \qquad [5]$$

and radiative capture

$$\sigma_\gamma(E) = 1 - |S|^2 - 2i(R^* - R)/|1 - iR|^2 \qquad [6]$$

in the model under consideration [4, 5].

By the average value of a certain physical functional F(R) we shall mean the result of the averaging F of both for an energy interval (group) which contains a large number of resonances and for the statistical distribution functions of the distribution of the x_λ and δ_λ parameters:

$$\langle F \rangle = \frac{1}{\Delta\varepsilon} \int d\varepsilon \prod_{\lambda} \int F(\varepsilon, x_1, x_2, \ldots \delta_1, \delta_2, \ldots) P(x_\lambda)\, dx_\lambda\, V(\delta_\lambda)\, d\delta_\lambda, \qquad [7]$$

where

$$P(x_\lambda) = \frac{1}{\sqrt{2\pi x_\lambda}} \exp(-x_\lambda/2) \qquad [8]$$

is the Porter-Thomas distribution [2]. For the δ_λ values we selected a Cauchy-type distribution:

$$V(\delta_\lambda)=\frac{\bar{\delta}}{\pi}\frac{1}{\delta_\lambda^2+\bar{\delta}^2} \qquad [9]$$

with a distribution width equal to δ / $-\infty < \delta_\lambda < \infty$.

Average total cross-section

Let us first find the average value exp(iRt) in our model

$$\langle e^{iRt}\rangle=\frac{1}{\Delta\varepsilon}\int d\varepsilon\prod_\lambda\int_0^\infty\frac{dx_\lambda}{\sqrt{2\pi x_\lambda}}\int_{-\infty}^{\infty}\frac{d\delta_\lambda}{\delta_\lambda^2+\bar{\delta}^2}\cdot\frac{\bar{\delta}}{\pi}\cdot\exp\left(\frac{ist x_\lambda}{\varepsilon+\pi\lambda+\delta_\lambda-iy}-\frac{x_\lambda}{2}\right)=$$

$$=\frac{1}{\Delta\varepsilon}\int d\varepsilon\prod_\lambda\left[1-2ist/(\varepsilon-\pi\lambda-iy')\right]^{-\frac{1}{2}} \qquad [10]$$

($y'= y+\delta$). The integral for δ_λ is solved by contour integration using the calculus of residues. In extending the summing for λ (3) from - ∞ to + ∞, let us take an infinite product formula (see [6] p. 51):

$$\prod_{\lambda=-\infty}^{\infty}\left(1-\frac{2ist}{\varepsilon+\pi\lambda-iy'}\right)=\frac{\sin(\varepsilon-iy'-2ist)}{\sin(\varepsilon-iy')}, \qquad [11]$$

then

$$\langle\exp(iRt)\rangle=\frac{1}{\pi}\int_{-x_2}^{x_2}d\varepsilon\sqrt{\frac{\sin(\varepsilon-iy')}{\sin(\varepsilon-iy'-2ist)}}=e^{-st}. \qquad [12]$$

In solving the integral by the calculus of residues we used the periodicity of the integrand, having substituted the energy averaging with a calculation of the average values for the period $-\pi/2 < \epsilon < \pi/2$.

The result obtained makes it possible to determine the average value of the functional $(1-iR)^{-1}$ in (5), using the integral identity:

$$\left\langle\frac{1}{1-iR}\right\rangle=\int_0^\infty dt\, e^{-t}\langle e^{iRt}\rangle=\frac{1}{1+s}\,. \qquad [13]$$

Consequently,

$$\langle S \rangle = e^{-2i\varphi} \frac{1-S}{1+S} \qquad [14]$$

and

$$\langle \sigma \rangle = 4 \left(\sin^2 \varphi + \frac{S}{1+S} \cos 2\varphi \right), \qquad [15]$$

which is completely analogous to certain formulae in reaction resonance theory for average scattering functions and averaged total resonance cross-sections [1, 2].

In a similar way it is not difficult to show that

$$\left\langle \left(\frac{1}{1-iR} \right)^m \right\rangle = \frac{1}{m!} \int_0^\infty t^m dt\, e^{-t} \langle e^{iRt} \rangle = \left(\frac{1}{1+S} \right)^m \qquad [16]$$

and

$$\langle S^m \rangle = e^{-2im\varphi} \left(\frac{1-S}{1+S} \right)^m, \langle S^{*m} \rangle = e^{2im\varphi} \left(\frac{1-S}{1+S} \right)^m. \qquad [17]$$

The agreement between the results achieved using our model and the general conclusions of R-matrix theory, where averaging of the S-matrix elements is equivalent to the transition to averaged elements $\langle R_{ps} \rangle = is\delta_{ps}$ in definition (1), illustrates the consistency of the approach and the potential for applying our model in the derivation of average cross-sections and also average resonance transmission cross-sections in filtered beams and group characteristics [7].

Average Capture Cross-Section

Let us represent the expression for the capture cross-section (6) in the form of a double integral:

$$\sigma_\gamma = -2 \int_0^\infty du\, e^{-u} \int_{-u}^{u} dv \frac{\partial}{\partial u} \exp \frac{1}{2} [R(u+v) - R^*(u-v)]. \qquad (18)$$

then, in order to calculate $\langle \sigma_\gamma \rangle$ it is necessary to find the average value

$$F(u,v) = \left\langle \exp \frac{1}{2} [R(u+v) - R^*(u-v)] \right\rangle = \frac{1}{\pi} \int_{-\pi/2}^{\pi/2} d\varepsilon \left[\frac{\sin(\varepsilon - iv) \sin(\varepsilon - iv)}{\sin(\varepsilon - ip) \sin(\varepsilon + iq)} \right]^{1/2}, \qquad (19)$$

where: $$p = f + sv,\ q = f - sv,\ f = \sqrt{s^2v^2 + 2syu + y^2}.$$

Here we have used the same scheme for reducing a multi- to a single-level integral scheme as in conclusion (12), disregarding fluctuations in level spacings, i.e. as an approximation of equivalent resonances. Such an approximation has no apparent effect on the calculation of average $\langle \sigma_\gamma \rangle$ values, which is shown by the results of the corresponding straightforward numerical calculations [3, 8].

Let us now determine the derivative

$$\frac{\partial}{\partial u} F = -sy \frac{sh\,2f}{2f} \Phi, \tag{20}$$

where

$$\Phi = \frac{1}{\pi} \int_{-\pi/2}^{\pi/2} d\varepsilon \frac{\sin^{1/2}(\varepsilon - iy)\sin^{1/2}(\varepsilon + iy)}{\sin^{3/2}(\varepsilon - iq)\sin^{1/2}(\varepsilon + iq)} = \frac{4}{\pi} \sqrt{\frac{sh(p+y)sh(q+y)}{sh^3(p+q)}}(1+k)E\left(\frac{2\sqrt{k}}{1+k}\right). \tag{21}$$

Here, E is an elliptic integral of the second kind, and

$$k = \left[\frac{sh(p-y)sh(q-y)}{sh(p+y)sh(q+y)}\right]^{1/2}. \tag{22}$$

As a result of his operation we obtain an expression for average cross-sections (18) in the form of a double integral

$$\langle \sigma_\gamma \rangle = 2sy \int_0^\infty du\, e^{-u} \int_{-u}^{u} \frac{dx}{f} \sqrt{\frac{sh(p+y)sh(q+y)}{sh(p+q)}} \frac{2}{\pi}(1+k)E\left(\frac{2\sqrt{k}}{1+k}\right), \tag{23}$$

where it is possible to use a straightforward interpolation formula for the elliptic integral which gives an error of less than 1% for $K \leq 1$ [9]:

$$\frac{2}{\pi}(1+k)E\left(\frac{2\sqrt{k}}{1+k}\right) \simeq 1 + \frac{k^2}{4} + \frac{k^4}{64}(1 + 0{,}48733k^2). \tag{24}$$

This result using our model to determine the average capture cross-section does not depend on the value of S, i.e. it is suitable for a random degree of resonance interference. Therefore it is obviously desirable to use the results of the calculation based on formula (2) in order to analyse the fluctuation correction to the average cross-section, which is calculated in a

Hauser-Feschbach approximation which does not give any allowance for resonance parameter fluctuation. For small values of S this correction is known and amounts to less than 35% [2, 3]. For random S values it can be determined by

$$F(s,y) = \langle \tilde{\sigma}_\gamma (s,y) \rangle / \bar{\sigma}_\gamma (s,y), \qquad (25)$$

where $\tilde{\sigma}_\gamma$ is calculated in a model of identical resonances.

In our approach, the identical resonance model is represented by an assumption of identical $x_\lambda = 1$ values in the determination of R(Є)(3) [2]:

$$\tilde{R} \approx s \sum_{\lambda=-\infty}^{\infty} \frac{1}{\varepsilon + x_\lambda - iy} = \pi s \operatorname{ctg}(\varepsilon - iy). \qquad (26)$$

then σ_γ represented by the integral:

$$\bar{\sigma}_\gamma = \frac{1}{\pi} \int_{-\pi/2}^{\pi/2} \left[1 - \left| \frac{1+i\tilde{R}}{1-i\tilde{R}} \right|^2 \right] d\varepsilon = \frac{4 s \operatorname{th} y}{(s + \operatorname{th} y)(1 + s \operatorname{th} y)}, \qquad (27)$$

which corresponds to the most elementary Hauser-Feschbach result for small values of $S = \pi\Gamma_n/2D$ and for $y = \pi\Gamma_\gamma/2D$ [1, 2].

The figure shows the results of the calculation of the F(s,y) function in our model for three values of S. Also given here are the data from our calculations of this function obtained earlier using the Monte Carlo method [4]. The good agreement illustrates the consistency of the proposed method, whose advantage, apart from the possibility of obtaining an analytic form σ_γ and the saving of computer time during the numerical calculations, lies in the potential for testing Monte Carlo data directly.

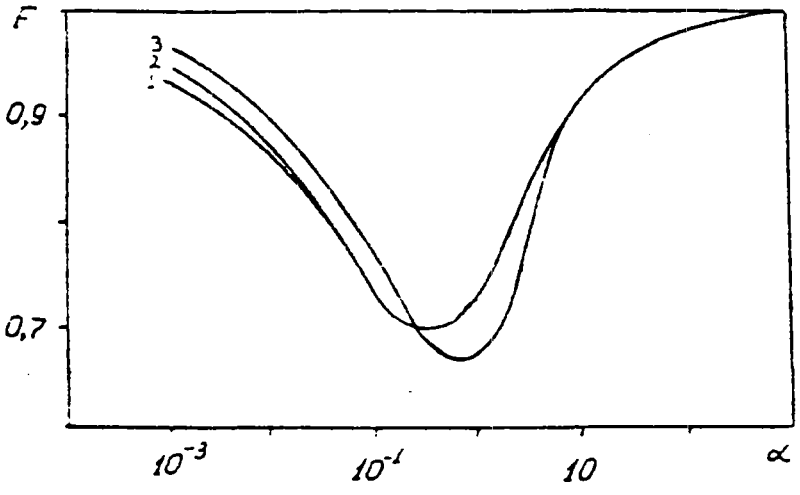

Function F, takes into account neutron width fluctuations in an average capture cross-section; it is expressed as a function of the $\alpha = y(1+S)^2/2S$ parameter for $S = 10^{-3}$ (1), 10^{-1} (2), 1 (3).

Appendix A. Integral (12)

When using the substitution u=tg ϵ, the integral (12), which occurs during calculation of $< \exp(iRt) >$, reduces to the form

$$I=\frac{1}{\pi}\int_{-\infty}^{\infty}\frac{du}{1+u^2}\sqrt{\frac{ch y'}{ch z}}\sqrt{\frac{u-i th y'}{u-i th z}}, \qquad (A.1)$$

where $z=y'+2st$. If we now close this integral in a complex plane with a semicircle of infinite radius downwards from the real axis, we will determine its value as the residue at the pole $u=-i$:

$$I=\sqrt{\frac{ch y'}{ch z}}\sqrt{\frac{1+th y'}{1+th z}}=e^{-st}. \qquad (A.2)$$

Appendix B. Form of Function F(u,v) (19)

Function F (19) is represented in the form of an integral in the following way:

$$F=<\exp\tfrac{i}{2}[(u+v)R-(u-v)R^*]>=$$
$$=\frac{1}{\Delta\epsilon}\int d\epsilon\prod_\lambda\int_0^\infty \exp\left[\frac{is}{2}\left(\frac{x_\lambda(u+v)}{\epsilon+\lambda\pi-iy}-\frac{x_\lambda(v-v)}{\epsilon+\pi\lambda+iy}\right)\right]P(x_\lambda)\,dx_\lambda= \qquad (B.1)$$
$$=\frac{1}{\Delta\epsilon}\int d\epsilon\prod_\lambda\left[1-is\left(\frac{u+v}{\epsilon+\lambda\pi-iy}-\frac{u-v}{\epsilon+\lambda\pi+iy}\right)\right]^{-1/2}=$$
$$=\frac{1}{\Delta\epsilon}\int d\epsilon\prod_\lambda\left(1-i\frac{p-y}{\epsilon+\lambda\pi-iy}\right)^{-\frac{1}{2}}\left(1+i\frac{q-y}{\epsilon+\lambda\pi+iy}\right)^{-\frac{1}{2}},$$

where

$$p=sv+f,\quad q=f-sv,\quad f=\sqrt{s^2v^2+2syu+y^2}.$$

Next, using the formula for infinite product (11) and substituting the energy averaging with the average period $-\pi/2 \le \epsilon \le \pi/2$, we obtain the integral form F(u,v) (19). This is the real function, which can also be represented in the form of a total elliptic integral of the third kind.

Appendix C. Integral (21)

Let us write the integral (21) in the form:

$$\Phi = \frac{1}{\pi} \frac{sh\,y}{sh^{1/2}p\, sh^{1/2}q} \int_{-\pi}^{\pi} \frac{dx}{\cos^2 x} \frac{\sqrt{1+tg\,x\,cth\,y}}{(cth\,p\,tg\,x-1)^{1/2}(cth\,q\,tg\,x+1)^{1/2}} \qquad (C.1)$$

and let us proceed to the variable $z - tg\frac{z}{2} = tg\,x\,cth\,y$. Then, having specified

$$th\varphi_1 = th\,y\,cth\,p,\ th\varphi_2 = th\,y\,cth\,q,\ m = \varphi_1 + \varphi_2,\ n = \varphi_2 - \varphi_1,$$

we can rewrite (C.1) to the form:

$$\Phi = \frac{\sqrt{2}}{\pi} \frac{sh\,y}{th^{1/2}y} \left(\frac{sh\,n}{sh\,2f}\right)^{1/2} \int_{-\pi}^{\pi} dz\,[ch\,m + \cos(z+in)]^{-\frac{1}{2}}. \qquad (C.2)$$

Using the identity:

$$\frac{1}{(a+\cos\eta)^{1/2}} = \frac{1}{a^2-1}\left[\sqrt{a+\cos\eta} - 2\frac{\partial}{\partial\eta}\frac{\sin\eta}{\sqrt{a+\cos\eta}}\right], \qquad (C.3)$$

by means of which using direct computation we obtain

$$\int_{-\pi}^{\pi} dz\,[ch\,m + \cos(z+in)]^{-1/2} = \frac{1}{sh^2 m}\int_{-\pi}^{\pi}\sqrt{ch\,m+\cos\eta}\,d\eta = \qquad (C.4)$$
$$= 4\sqrt{2}\,(ch\,\tfrac{m}{2}/sh^2 m)\,E(ch^{-1}\tfrac{m}{2}),$$

where E is a total elliptic integral of the second kind [6]. By substituting (C.4) for (C.2) and denoting the parameter

$$k = e^{-m} = \sqrt{\frac{sh(p-y)sh(q-y)}{sh(p+y)sh(q+y)}}, \qquad (C.5)$$

so that

$$1-k^2 = \frac{sh\,2f\,sh\,2y}{sh(p+y)sh(q+y)}, \qquad (C.6)$$

we come to the representation of Φ which we obtained in (21).

REFERENCES

[1] LANE,A., THOMAS, R., "Nuclear Reaction Theory at Low Energies Inostrannaya Literatura, Moscow (1960). [Tranl. from Engl.]
[2] LUKYANOV, A.A., Neutron Cross-sections, Atomizdat, Moscow (1978) [in Russian].
[3] TEPEL, J.W., HOFFMANN, H.M., WEIDENFULLER, H.A., Phys. Lett. 498 (1974) 1.
[4] LUKYANOV, A.A., YANEVA, N.B., Sov. Journ. Nucl. Phys. 42 (1985) 1376.
[5] JANEVA, N.B., et al., Fluctuation Factors of Averaged Cross-sections in Overlapping Resonances, in Proc.Int. Conf. Santa Fe, New Mexico, 2 (1985) 1615.
[6] GRADSTEIN, I.S., RYZHIK, I.M., Tables of Integrals, Sums, Series and Products, Fizmatgiz, Moscow (1962). (in Russian)
[7] LUKYANOV, A.A., Moderation and Absorption of Neutron of Neutron Resonances, Atomizdat, Moscow (1974) [in Russian].
[8] KUYUMDZHEVA, N., YANEVA, N.B., Voprosy atomnoy nauki i tekhniki. Yadernye Konstanty, Ser. 3(42) (1981) 88 [in Russian].
[9] DWIGHT, G.O., Tables of Integrals, Nauka, Moscow (1964).

Submitted for publication 23 May 1988

APPLICATION OF THE INCREMENTAL DECONVOLUTION METHOD TO ANALYSE DELAYED NEUTRON INTENSITY DECAY CURVES

S.V. Krivasheev

ABSTRACT

In order to evaluate the cumulative yields of the main precursors of delayed neutrons, it is proposed that the incremental deconvolution method be used to analyze the experimental data of the delayed neutron intensity decay curves. The advantages of this approach are illustrated for thermal neutron fission of ^{233}U and ^{235}U.

As was shown in Reference [1], the incremental deconvolution method [2] can be applied to the decomposition of spectral multiplets into their components in a composite amplitude spectrum. Using the incremental deconvolution method, the iteration algorithm for finding an approximate solution to the system of equations

$$A(i) = \sum_{j=1}^{M} B(j) F(i,j), \quad i = 1, \ldots, N, \qquad (1)$$

(where A(i) is the observed spectrum, N is the number of experimental points, B(j) is the real spectrum, M is the number of unknown components, and F(i,j) is the instrumental form of the line) consists only of addition and subtraction operations, and is therefore expedient for processing on a microcomputer. Additional advantages of the method are that the unknown parametrization coefficients B(j) in equation (1) are positively constraint as required when dealing with many physical problems, and there is no need for initial approximations ($B_0(j) = 0$), thereby eliminating subjectivity from the analysis of experimental data. As will be shown below, the incremental deconvolution method can be used to analyse delayed neutron intensity decay curves derived from an unseparated mixture of fission products in the determination of the cumulative yields of

individual precursors. It should be noted that in the given case, the least squares method is not suitable for solving equation system (1) because there is no positivity constraint when a large number of parameters are being determined. Furthermore, the error matrix is badly conditioned.

By definition, the following relationship is valid for a given delayed neutron precursor:

$$Y^n(j) = Y^c(j) P_n(j), \qquad (2)$$

where $Y^n(j)$ is the delayed neutron yield from a precursor with index j, $Y^c(j)$ is its cumulative yield, and $P_n(j)$ is the probability of neutron emission by a daughter nucleus of the precursor.

In the given case, the B(j) coefficients from Eq. (1) are equal to $Y^n(j)$ which has an accuracy which includes the number of fissions in the sample for per unit time and the detector efficiency. F(i,j) is the time dependent function describing the delayed neutron decay in successive time intervals and is dependent on the experimental conditions [3], consisting of repeated cyclical neutron irradiation of the sample, transfer of the container with the sample to the measuring position by a pneumatic transport system and measurement of the delayed neutron intensity itself with respect to time using a neutron counter.

At the present time, approximately 200 delayed neutron precursors are known. However, by subdividing them according to their half-lives $T_{1/2}(j)$, we find that the main contributors to the delayed neutron intensity originate from long-lived precursors with $T_{1/2} \geq 2$ s. These consist of 9 to 12 nuclides depending on the fuel type (see Table 1). The data in Table 1 are based on studies reported in Refs [4, 5]. The contribution of other precursors, not included in Table 1, to the delayed neutron yield for the four long-lived groups of the conventional six time groups [6] is less than those given in the table. Our purpose in selecting the ^{249}Cf, ^{235}U, and ^{236}U nuclei for analysis

of the delayed neutron contributing nuclides was to show that in the broad range of fissile actinides at various neutron energies, the set composition of the main precursors remains roughly the same.

Thus, the integral delayed neutron intensity decay curve can be analysed for nine (M = 9) main contributors with account taken that in the time it takes to transfer the sample from the irradiation to the measuring position (namely, approximately 2 s), the short-lived fission products would have already decayed . As a rule, the yield of the delayed neutron group for which $T_{1/2}$ = 2 s should not be attributed to any particular precursor since the group includes ^{90}Br, ^{85}As and other nuclei with shorter half-lives.

The authors of Ref. [8] were the first to show that the integral curve of delayed neutron intensity decay can be broken down into yields from individual precursors using the method of least oriented divergence. This method is analysed in parallel with the incremental deconvolution method below.

We need to check that the integral curve of delayed neutron intensity decay can actually be subdivided according to their half-lives $T_{1/2}(j)$, as shown in Table 1. In doing this, we obtain randomized curves for distinct real experiment statistics and a selection of precursors. The pseudo-experimental points were a sampling from a Poisson distribution. Since the incremental deconvolution method (like most iteration methods) does not permit evaluation of the B(j) error values, the recommended curves were modelled several times for the same statistic. In order to evaluate the error, unbiased sampling dispersions were taken for similar measurements with allowance given for Student coefficients for a confidence level of 0.70 and the given number of degrees of freedom. The results are given in Table 2. Analysis of these results yields the following conclusions. First, in order to obtain unbiased evaluations for the values of B(j) we need to increase the number of evaluated curves and experiment statistic; in practice this means increasing the number of experiment cycles, as discussed earlier, and also

increasing the mass of the measure sample and the density of the neutron flux. Second, in order to reduce the error in determining B(j) for long-lived delayed neutron precursors we need to increase the irradiation time of the measured sample, and correspondingly similarly reduce it for short-lived precursors. Otherwise, we cannot include exponential curves with $T_{1/2}(j) \approx 5$ s or less.

The incremental deconvolution and least oriented divergence methods were investigated jointly on three pseudo-experimental curves obtained for 68 delayed neutron precursors, including short-lived nuclides ($T_{1/2}(j) \approx 0.8$ s), for thermal neutron fission of ^{235}U. From Table 3 it can be seen that the least oriented divergence method yields more biased evaluations ($\sim 3\sigma$) than the incremental deconvolution method although it has great resolution stability. During the checking of the methods it was found that the least oriented divergence method was neither as efficient (the method converges quickly only in the first iteration steps) or as fast-acting as the incremental deconvolution method. The incremental deconvolution method was also verified using real experimental data (obtained using the method described in Ref. [3])for thermal neutron fission of ^{235}U and ^{233}U, , with admissible statistics and a number of analysed curves. The ^{235}U and ^{233}U nuclides were selected because of the reliability of the known cumulative yields of the delayed neutron precursors. Since the values of $Y_n(j)$ derived from the analysis of the experimental curves are accurate to within a constant multiplier factor, referred to earlier, normalization was carried out using the total relative yields of the five delayed neutron groups in the evaluation of the same curves by the least squares method for 5-group approximation and the corresponding recommended values given in Table 4. There was satisfactory agreement within the error margin between the cumulative yields measured here and those recommended in Ref. [4]. It should be noted that minor deviations in the measured yields might result from the fact that no account was taken of the decay dynamics of the precursor nuclides with their parent nuclide having a half

life longer than 3 s, as this would have doubled the number of parameters to be determined. Evaluations of this phenomenon indicate that with the exception of ^{238}U and ^{232}Th fission[7], the results may have an error of up to 5%.

Table 1

Calculation of delayed neutron yields from individual precursors per 10^4 fissions

j	1	2	3	4	5	6
1	^{83}Br	55.7	2.54±0.10	0.31	5.4	4.2
2	^{137}I	24.5	7.2±0.7	5.8	24.0	16.0
3	^{136}Te	19.0	0.9±0.4	0.11	1.4	0.6
4	^{88}Br	16.0	6.9±0.3	0.57	15.6	11.5
5	^{103}Nb	15.7	0.13±0.00*	0.28	0.32	0.13
6	^{138}I	6.5	2.6±0.3	0.52	4.4	2.6
7	^{93}Rb	5.86	1.37±0.08	0.47	4.5	4.4
8	^{89}Br	4.38	13.9±1.0	0.49	24.9	19.2
9	^{97}Y	3.7	0.33±0.00	0.36	1.7	1.6
10	^{94}Rb	2.76	10.3±0.5	1.4	22.6	21.1
11	^{139}I	2.38	10.2±0.9	0.44	6.5	3.8
12	^{85}As	2.03	22.0±8.0	0.06	5.7	5.5
13	^{98}Y	2.00	0.54±0.00	0.39	2.0	0.82
14	^{90}Br	1.80	21.2±2.4	0.30	17.4	12.1
15	^{143}Cs	1.78	1.6±0.2	0.01	0.29	0.06
16	^{99}Y	1.40	1.2±0.8	0.44	2.7	2.5
Total contribution of delayed precursors				A	B	C
% of delayed neutron yield for four groups				71	91	92

1 - Precursor nucleus

2 - $T^{1/2}$ (j), sec.

3 - $P^n(j) \pm \Delta P^n(j)$, %

4 - ^{249}Gf (T), $Y_{(j)}{}^n(j)$

5 - ^{235}U (F), $Y_{(j)}{}^n(j)$

6 - ^{236}U (NF), $Y_{(j)}{}^n(j)$

* - $P_n(j=5)$ value from Ref.[7]

A - 12.0±3.0

B - 139.4±16.0

C - 105.9±11.4

T - thermal neutron fission

F - fast neutron fission

NF - 14.8 MeV neutron fission

Table 2

Analysis of randomized delayed neutron curves using the incremental deconvolution method

P	1		2		3	
	T	V	T	V	T	V
^{87}Br	1300	1289±56	130	144±6	130	189±44
^{137}I	7952	7679±212	795	738±25	795	643±144
^{88}Br	4241	4736±249	424	495±46	424	566±151
^{138}I	3344	2966±375	334	307±94	334	294±106
^{93}Rb	1675	1769±69	167	155±52	167	126±79
^{89}Br	6872	6387±480	687	666±164	687	641±129
^{94}Rb	6405	8017±909	640	700±133	640	958±253
^{139}I	3841	3470±693	384	413±137	384	304±117
A	6573	5459±1443	657	509±157	657	483±363
B	32	32	32	32	32	32
C	20000		3000		1900	
D	10		60		10	
E	5		5		5	

P - Delayed neutron precursor
A - ^{90}Br, ^{85}As and others
B - Background
C - Radiometer capacity, n/s
D - Irradiation duration, s
E - Number of curves
T - values of B(j) prescribed by the curve modelling
V - values of B(j) derived from curve evaluation

Table 2(continued)

P	4		5	
	T	V	T	V
^{87}Br	3250	3210	-	-
^{137}I	19880	19980	-	-
^{88}Br	10604	10580	-	-
^{138}I	8360	7245	-	-
^{93}Rb	4188	6948	-	-
^{89}Br	17182	13700	-	95±58
^{94}Rb	16014	18320	4804	3970±208
^{139}I	9603	10450	2880	2578±1284
A	16434	14010	4930	5953±1182
B	80	80	24	24
C	26000		3000	
D	60		60	
E	1		5	

P - Delayed neutron precursor
A - ^{90}Br, ^{85}As and others
B - Background
C - Radiometer capacity, n/s
D - Irradiation duration, s
E - Number of curves
T - values of B(j) prescribed by the curve modelling
V - values of B(j) derived from curve evaluation

Table 3

Analysis of randomized curves using the incremental deconvolution and best directed discrepancy method

A	B	C	D	E
^{87}Br	55.7	1564	1571±60	1739±34
^{137}I	24.5	7093	7189±191	6415±62
^{88}Br	16.0	3639	4359±254	5058±28
^{138}I	6.5	2508	1834±927	2581±32
^{93}Rb	5.86	1444	1598±264	2597±20
^{89}Br	4.38	5156	5392±1721	2915±15
^{94}Rb	2.76	4804	7882±1059	4195±64
^{139}I	2.38	2881	2347±1074	4799±79
F	2.0	5800	3986±1286	5636±122
G	0.8	6200	7667±3499	11990±1234
H	∞	24	24	24

A - delayed neutron precursor
B - Half-life $T_{½}(j)$, s
C - Incremental deconvolution method B(j), T
D - Least oriented diversion method 'B(j)
E - MNNP "B(j) method
F - ^{90}Br, ^{85}As and others
G - ^{144}Cs, ^{100}Y and others
H - background

Table 4

Results of the determination of the cumulative yields of delayed neutron precursors

Delayed neutron precursor	^{235}U		^{233}U	
	This work	[4]	This work	[4]
^{87}Br	2.21±0.32	2.02±0.06	2.33±0.39	2.16±0.13
^{137}I	3.10±0.53	3.33±0.13	1.76±0.33	1.66±0.07
^{88}Br	2.17±0.34	1.91±0.11	1.12±0.24	1.32±0.11
^{138}I	2.12±0.48	1.56±0.09	0.84±0.28	0.59±0.09
^{93}Rb	3.68±0.60	3.54±0.05	2.58±0.64	2.11±0.49
^{89}Br	1.17±0.23	1.18±0.05	0.75±0.17	0.65±0.05
^{94}Rb	1.77±0.37	1.69±0.05	0.64±0.23	0.65±0.42
^{139}I	1.00±0.20	0.96±0.03	0.21±0.07	0.21±0.09
Normalized yield	1.58±0.04		0.67±0.04	

REFERENCES

[1] KOVALENKO, V.V., "Automation of Physical Investigations", Ehnergoatomizdat, Moscow (1984) 173 [in Russian].
[2] KENNET, T.J., PRESTWICH, W.V., Nucl. Instr. Meth. 203 (2982) 317.
[3] GUDKOV, A.N., ZHYVIN, V.M., KOVALENKO, V.V., et al., Vopr. At. Nauki i Tekhn., Ser. Yadernye Konstanty 2 (1986) 56 [in Russian]
[4] RIDER, B.F., Compilation of fission product yields, Report NEDO-12154-3(B), Vallecitos Nuclear Center (1980).
[5] ENGLAND, T.R., WILSON, W.B., SCHENTER, R.E., MANN, F.M., Nucl. Sci. Eng. 85 (1983) 139.
[6] KEEPIN, G.R., WIMETT, T.F., ZIEGLER, R.K., J. Nucl. En. 57 (1957) 1.
[7] MANEVICH, L.G., NEMIRVSKIJ ,P.Eh., YUDKEVICH, M.S., Delayed neutron constants, Preprint IAEh-4308/4, Moscow (1986) [in Russian].
[8] TARASKO, M.Z., MAKSYUTENKO, B.P., Yad. Fiz. 17 (1973) 1149. (Engl. transl.: Sov. J. Nucl. Phys. 17 (1973) 598).
[9] SHIMANSKIJ, A.A., TARASKO, M.Z., Speeding up the iteration process in the least oriented divergence method, Preprint FEhI-791, Obninsk (1977) [in Russian].
[10] KENNET, T.J., PRESTWICH, W.V., ROBERTSON, A., Nucl. Instr. Meth. 151 (1978) 285.

Submitted for publication 19 May 1988

DERIVATION OF THE STATISTICAL CHARACTERISTICS OF THE ENERGY DEPENDENCE OF TOTAL NEUTRON CROSS SECTIONS FROM TRANSMISSION DATA IN SAMPLES OF VARYING THICKNESS

V.K. Basenko, G.A. Prokopets

ABSTRACT

A new approach to process neutron transmission experimental data in the unresolved resonance energy region is described. The efficiency and reliability of the method is demonstrated for several cases. The process consists of deriving the statistical characteristics of the total cross-section energy dependence from transmission data in samples of various thicknesses. The results of this process are compared with other known approaches to this problem.

The analysis of the continuous neutron transmission spectrum as a function of sample thickness has long been used successfully together with high resolution experimental data to derive group data for reactor physics [1-3]. At the same time we know that as neutron energy increases, the counting equipment resolution ΔE becomes too poor to identify the resonance structure reliably, consequently, experimental transmission data assumes greater importance as a source of information to determine average characteristics of the energy dependence of the total cross sections in the ΔE energy interval.

For a collimated neutron beam with an energy density distribution $\varphi(E)$, transmission in a sample $T(y)$ of thickness d and nuclear density N is determined as follows

$$T(y)=\int_0^\infty P(E)\exp[-y\sigma_t(E)]\,dE,$$

where $y = nd$,

$$P(E) = \varphi(E)/\int_0^\infty \varphi(\epsilon)\,d\epsilon$$

whole region for which values are being determined. This task is made significantly easier by the fact that even in the case of a fast oscillating dependence of $\sigma_t(E)$, the function T(y) remains fairly smooth. When the experimental results for $\sigma_{eff}(y_i)$ are presented in the form

$$T(y_i) = \exp[-y_i \sigma_{эф}(y_i)], \tag{5}$$

they tend to follow curves of a low order with respect to y. Therefore, it is useful to perform numerical differentiation and integration in expressions (3) and (4) by approximating the discreet set $\sigma_{eff}(y_i)$ with a suitable analytic expression which takes account of the physical requirements which condition its shape in the vicinity of $y \to$ and $y \to \infty$. These requirements include that

(a) $\sigma_{eff}(y)$ is finite and positive over the whole range in which values are being determined, including $y \to 0$ and $y \to \infty$;

(b) the following condition is satisfied

$$\lim_{y \to \infty} \sigma_{эф}(y) = \sigma_{t\,min}, \tag{6}$$

where σ_{tin} is the lowest value of the total interaction cross section in the averaging range, so that

$$\lim_{y \to \infty} \frac{\partial \sigma_{эфф}(y)}{\partial y} = 0; \tag{7}$$

(c) It shows from expression (3), that the semi-invariance of the total cross section when averaging over the ΔE range will be simply expressed by the derivatives of $\sigma_{eff}(y)$ at zero:

$$æ_{\nu+1} = (-1)^{\nu} \cdot (\nu+1) \lim_{y \to 0} \frac{\partial^{\nu} \sigma_{эфф}(y)}{\partial y^{\nu}}; \quad \nu \geq 0. \tag{8}$$

In particular, $æ_1 \equiv \langle \sigma_t \rangle = \sigma_{эфф}(0)$; $æ_2 \equiv \gamma_{\sigma_t} = -2 \frac{\partial \sigma_{эфф}(0)}{\partial y}$,

and $\sigma_t(E)$ is the total interaction cross-section for neutrons of energy E with nuclei in the sample. If we further assume that the energy distribution $\varphi(E)$ is suitably narrow, i.e. that its width at half maximum of ΔE is significantly lower than the characteristic range in the variation of the neutron detector efficiency, we can equate the transmission level value, as given by Eq. (1), with the experimental difference between the neutron counting rate without sample in the beam and the counting rate with the sample. The energy shift caused by the inelastic scattering in the sample causes a noticeable increase in ΔE, and necessitates the usual corrections for scattering in the detector. It is clear from equation (1) that, by measuring the transmission level T for different thicknesses y and, therefore, assuming the function T(y) to be known, we can immediately correlate the results of such measurements with the whole set of initial values

$$\langle \sigma_t^{\nu} \rangle = \int_0^{\infty} P(E) \sigma_t^{\nu} dE, \tag{2}$$

which characterize the energy dependence of the total neutron cross sections in the ΔE(ν = 0,1,2,3,...).

$$\langle \sigma_t^{\nu} \rangle = (-1)^{\nu} \lim_{y \to 0} \frac{\partial^{\nu} T(y)}{\partial y^{\nu}}; \quad \nu \geq 0, \tag{3}$$

$$\langle \sigma_t^{\nu} \rangle = \frac{1}{(|\nu|-1)!} \int_0^{\infty} y^{|\nu|-1} T(y) dy, \quad \nu < 0 \tag{4}$$

What follows relates to the algorithm of the calculations based on equations (3) and (4).

The experimental data is available in the form of a discreet set of values of $K(y_i)$ obtained for a finite number M of y_i values. This set does not include the extreme points y = 0 and y = ∞ or the points lying close to them. Thus, we can only use expressions (3) and (4) to find $\langle \sigma_t^{\nu} \rangle$ by extrapolating the behavior of $T(y_i)$ in the measured range of y_i values over the

which means that the first derivative at zero cannot be positive:

$$\frac{\partial \sigma_{эфф}(0)}{\partial y} \leq 0. \qquad (9)$$

Since expression (4) must be numerically integrated to find the "inverse" momenta of the cross section ($\nu < 0$), it is desirable to replace the variable y with the variable z which approaches a finite limit when $y \to \infty$ and would automatically ensure that condition (7) is satisfied at infinity. We chose the following transform for the variables

$$z = \frac{2}{\pi} arctg(\lambda y), \qquad (10)$$

where $\lambda > 0$ and

$$\lim_{y \to 0} z(y) = 0 \; ; \; \lim_{y \to \infty} z(y) = 1. \qquad (11)$$

This means that condition (7) is fulfilled since
Another advantage of the transform given by equation(10) is the possibility of approximating σ_{eff} with orthogonal polynomials using a finite orthogonalization interval:

$$\sigma_{эфф}(\lambda, z) = \sum_{k=0}^{k_{max}} A_k(\lambda) T_k^*(z). \qquad (12)$$

where $T_k^*(z) = \sum_{j=0}^{k} \beta_j^{(k)} \cdot z^j$ is the displacement of the Chebyshev polynomial. The approximation parameters λ, A_k, k_{max}, which are determined using the least squares method, usually satisfy the conditions set out under points A-C. Using the conditions set forth in equations (3, 4, 6, 8), the functions $\sigma_{eff}(1,z)$ determined in this way can be used to produce data, on the statistical characteristics of the energy dependence of the total neutron cross sections such as the set of "direct" ($\nu \geq 0$) and "inverse" ($\nu < 0$) initial or central conditions, as well as σ_{tmin}. The uncertainty of the coefficients A_k and, similarly, that of the derived coefficients are obtained in the usual way using the error matrix.

We checked the objectivity and accuracy of this method to derive the statistical characteristics of the energy dependence of the total neutron cross sections from data on the transmission for varying sample thicknesses, by performing inverse convolution of the real excitation functions $\sigma_t E$ obtained under high resolution conditions, and beams in the form of a Gaussian function or a square pulse of width ΔE given by expression (1) in order to generate the transmission function T(y). The experimental error were simulated by a random distribution of sample values within a 3% error range which is typical for transmission measurements. The excitation functions were taken from the KFK-1000 reference. For some of these excitation functions, the statistical characteristics obtained by direct averaging of $\sigma^{v}_{t}(E)$ using equation (2) were compared with those obtained from an analysis of the model transmission levels. A typical result of this kind of comparison is given in Table 1.

Data on $\sigma_t E$ for natural chromium isotope mixture in the $750.1 \leq E \leq 889.7$ keV and $905.2 \leq E \leq 1049.9$ keV energy range were used. Figure 1 shows the corresponding portions of $\sigma_2(E)$. In both cases, the parameter K_{max} in Eq. (12) which ensures a minimum χ^2 value, was $K_{max} = 3$. As can be seen, the level of agreement is on the whole good and breaks down only for the semi-invariance κ_υ where $\upsilon \geq 3$, namely when the inverse momenta are reproduced usually up to a value of $|\upsilon| = 5$. There is also a tendency to overestimate of the minimum cross section σ_{tmin} in the range of values derived from the analysis of the transmission T(y).

In order to improve the determination of σ_{tmin}, and in view of the need to find such an important value as the highest total cross-section value σ_{tmax} in a given range, the transmission data processing procedure was extended to include an approximate calculation of the probability density function $\varphi(x)$ to determine the probability of observing in the ΔE range the value

$$x = \alpha \cdot (1/\sigma_t) - \beta, \qquad (13)$$

where $\alpha = \frac{2\sigma_{t\max}\sigma_{t\min}}{(\sigma_{t\max} - \sigma_{t\min})}$; $\beta = \frac{\sigma_{t\max} + \sigma_{t\min}}{\sigma_{t\max} - \sigma_{t\min}}$.

Without loosing any generality, $\varphi(x)$ can always be represented in the form of a polynomial

$$\varphi(x) = \sum_{\ell} B_\ell P_\ell(x), \qquad (14)$$

where $P_\ell(x)$ are Legendre polynomials. The coefficients B_ρ can now be calculated starting with the condition of non-negativity of $\varphi(x)$ at all points in the region where x is to be determined and the reproduceability of the full set of previously determined "direct" ($\upsilon \geq 0$) and "inverse" ($\upsilon < 0$) momenta $< \sigma_{\upsilon t} >$. In particular, by determining the variable x in the form given in Eq. (13) we can produce a simple algorithm for calculating B_ρ for inverse momenta since $B_\ell = \frac{2\ell+1}{2} < P_\ell(x) >$. Then the number of members in the polynomial given by the series (14) is limited by the number of non-inverse momenta so that, usually, $\rho_{max} \leq 5$. The condition of the non-negativity of $\varphi(x)$ and the reproducibility of the first direct momenta of the cross-section calculated using $\varphi(x)$ are fulfilled by varying the parameters d and β which means we can then find σ_{tmin} and σ_{tmax}. Figure 2a shows the probability density function $\varphi(1/\sigma_t)$ determined in this manner which was obtained by modelling T(y) using experimental $\sigma_t(E)$ data for chromium in the $1074.1 \leq E \leq 1204.8$ keV energy range alongside the distribution directly calculated for this section of the excitation function (histogram). If we take into account the non-smooth nature of the experimental distribution which was obtained from a finite number of intervals we may judge the general level of agreement of both distributions to be satisfactory. This is especially so when we compare the derived values of σ_{tmin} and σ_{tmax} with their real values (see Table 1). However, despite the generality of the method used, the limited number of determined momenta and their possible error levels in some cases means that we cannot find values of σ_{tmin} and σ_{tmax} which satisfy the condition of non-negativity of $\varphi(x)$. Therefore, we

also tried finding $\varphi(\sigma_t)$ via a priori specification of the type of distribution. Use of the two parameter β distribution whose parameters are fixed only by the $< \sigma_t >$ and $D\sigma_t$ values, yields good results (see Figs 2b, 3). The quality of the reproduction of the total set of inverse momenta and σ_{tmin}, σ_{tmax} is approximately the same as in the first example. One positive point is that the difficulty in realizing the positivity of $\varphi(x)$ associated with expression (14) does not occur here; however, this is achieved at the cost of less generality since the question as to how applicable the β distribution is to an analysis of a sufficiently extensive set of types of excitation function has not been investigated. It should be stressed that we only use the concept of probability density for the cross-section in the averaging interval when we are deriving the single characteristic σ_{tmax}; data on the momenta $< \sigma^{\nu}_t >$ are derived independently directly from the transmission data T(y). In contrast to other sources [2, 5], we set the cross-section distribution function for the range $\sigma_{tmin} \leq \sigma \leq \sigma_{tmax}$ and not for the $0 \leq \sigma < \infty$ region which does not exclude the possibility of observing very high cross-section values or unjustifiably low values with a finite probability within the limits of ΔE. Another advantage of this method is the simplicity of the algorithm which eliminates the need to numerically solve the integral equations in Ref. [2] and the instabilities associated with this, or the need to turn to a specific theoretical model [3,4]. Furthermore, with respect to any influence that the beam shape P(E) might have on the derived values for $< \sigma^{n}_t >$, we checked this in the calculations for two cases: an even distribution with a width of ΔE and a Gaussian shape with the same width at half maximum. The differences were no more than 1%.

The transmission curve processing method was then applied to real experimental transmission data T(y). Data for natural uranium were chosen for comparison. Uranium has been fairly extensively studied from the point of view of a knowledge of its group constants in the badly resolved resonance region

$2 \leq E \leq 100$ keV. However, even here the effect of the spread of the data from various sources on the average group total cross-sections exceeds the error levels given and the differences for the resonance self-shielding factors can be as high as several tens of percent (see Refs [5,6], for example). To a large extent this is linked to the behavior of the experimental transmission values at very small thicknesses ($d < 0.5$ cm) where there are major technical difficulties in carrying out the measurements.

Therefore, since our main aim was to check the adequacy of our procedure for analyzing transmission data, we selected the data from Ref. [5] which were obtained over a wide range of thicknesses $d > 0.5$ cm where the results from various sources agree overall. In the original, these data were processed using the method of least directed divergence [2]. Table 2 gives the uranium group constants which we derived and the results obtained by analyzing the original source [5] and the recommendations in ABBN-78 [7].

Figure 3 illustrates a type of derived total cross-section density distribution $\varphi(\sigma_t)$ for the second group (σ_{tmin} = (7.0 $\pm$ 0.3) barns; σ_{tmax} = (45 $\pm$ 4) barns) alongside the one obtained in Ref. [5]. The level of agreement is in all cases entirely acceptable. An analogous comparison was also carried out for the data on the transmission of quasi-monochromatic beams of fast neutrons in a natural chromium isotope mixture obtained in Ref. [8]. This element is also important in nuclear power technology. Table 3 gives the results for two average neutron energy values $< E >$. The widths ΔE of the energy distribution of the incident beam at half maximum are also given.

The energy dependences of the mean total cross-sections for chromium and of the self-shielding factors in the $0.49 \leq D \leq 1.355$ MeV region, which we obtain by analyzing the transmission values in Ref. [8], are shown in Fig. 4 alongside the results from Ref. [8]. As we can see, the differences in the

$< \sigma_t >$ values found using these two analysis techniques comprise on average ~5%. The anomalously high difference at the point $< E > = 0.553$ MeV was mainly caused by the relatively poor quality of the experimental source data together with the excessively small beam width. If we exclude this point, the differences in the derived total cross-sections would be on average around 3%. On the other hand, the values which we obtained for $< \sigma_t >$ are a little higher than those given in Ref. [8] at lower energies and rather lower in the upper part of the energy region. The F_t values differ on average by ~4%, mainly owing to the fact that our values are slightly higher than the ones given in Ref. [8] for E > 1 MeV. Upon averaging of the group intervals (ABBN groupings [7]), our results agree quite well with the data given in Ref. [9] produced using the analysis technique from Ref. [3], and with the data in Ref. [10] which were produced using the analysis technique from Ref. [2] (see Table 4).

The observable differences are less than 10% and reflect the need to further refine the group data of chromium.

With respect to the calculations which use the experimental data on the detailed dependence of $\sigma_t(E)$, as we can see from Fig. 4 which shows the values of $<\sigma_t>$ and F_t obtained by averaging the KFK-1000 values in the same intervals as the transmission data which we analysed from Ref. [8], the cross-sections are on average lower and the shelf-shielding factors higher than those derived from transmission experiments. As a rule, this indicates resonance omission and smoothing of the minima as a result of the finiteness of the energy resolution in the $\sigma_t(E)$ measurements.

Owing to the simplicity of the algorithms used, the calculations could be performed on a small SOU-1 computer with about the same memory, capacity and speed as the well-known Ehlektronika-60. The operating programs were written in BASIC, and the calculation time for the momenta $<\sigma^{\nu}_t>$ from the transmission data was 2-3 minutes. It took approximately 30

minutes to determine σ_t min and $\sigma_{t\ max}$. In conclusion, we may claim that the technique which we put forward here for deriving the statistical characteristics of the energy dependence of total neutron cross-sections from data on transmission levels in samples of varying thickness is sufficiently objective and accurate.

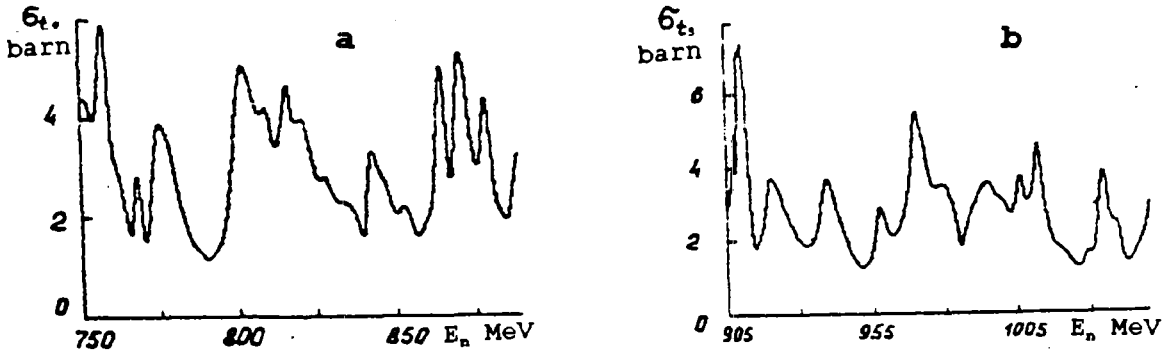

Fig. 1. Energy dependence pof the total neutron cross-sections of chromium in the 750.1 ≤ E ≤ 889.7 keV energy range (a), and in the 905.2 ≤ E ≤ 1049.9 keV energy range (b). (Data from KFK-1000)

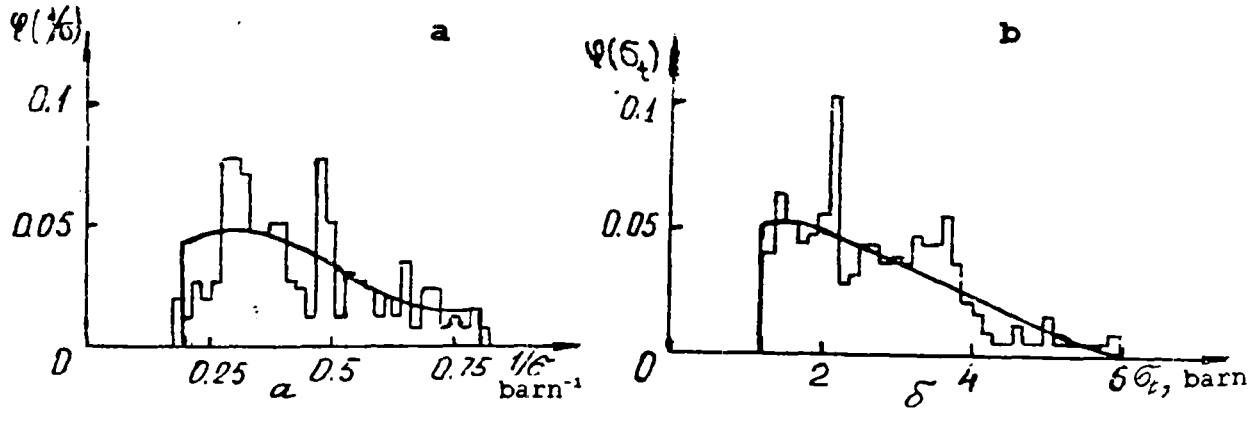

Fig. 2. Density distribution (a) $\varphi(1/\sigma_t)$ and (b) $\varphi(\sigma_t)$ for chromium in the 1074.1 ≤ E ≤ 1204.6 keV energy interval. The histogramshows results obtained via direct counting using the experimental excitation function; the continuous line shows results obtained via calculations using the method described.

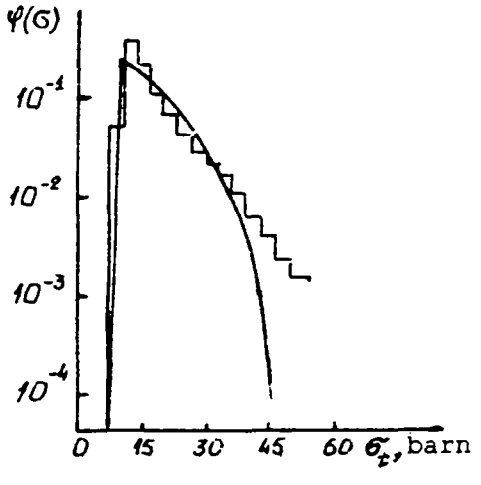

Fig. 3. Density distribution $\varphi(\sigma_t)$ for uranium (Group II). Histogram data from Ref. [3]; continuous line from calculation using described method.

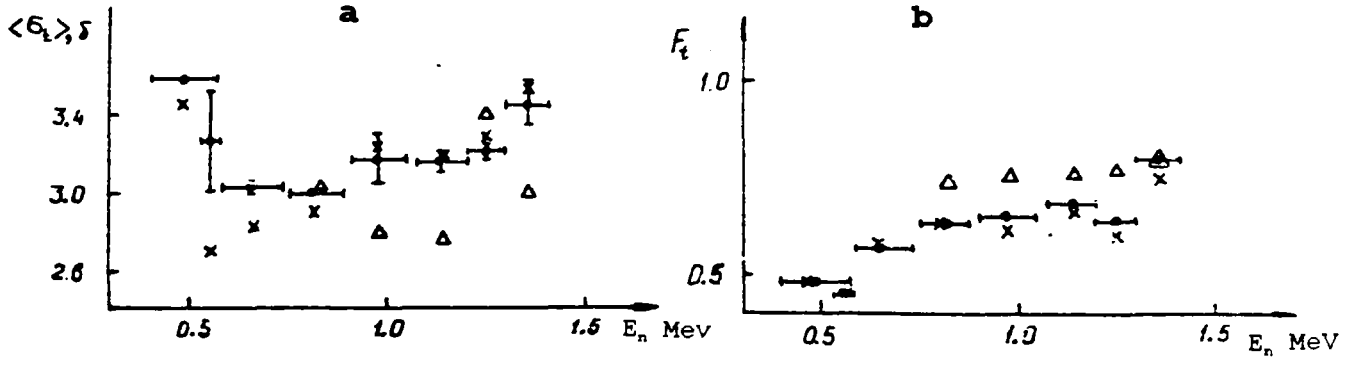

Fig. 4. (a) average cross-sections $\langle\sigma_t\rangle$, and (b) resonance self-shielding factors F_t for chromium in the $490 \leq E \leq 1355$ keV energy range: ⊢⊣ our data; x data from Ref. [8]; ▲ average of data from KFK-1000.

Table 1

Statistical characteristics of the energy dependence of the total chromium cross-section derived from high resolution data.

Characteristics	750.1 < E < 889.7 keV		905.2< E < 1049.2 keV	
	1	2	3	4
$<\sigma_t>$, δ	3.028	3.036±0.005	2.788	2.787±0.001
$D\sigma_t$, δ	1.205	1.26±0.01	1.201	1.143±0.007
$\mu\sigma_t$, δ	0.453	0.75±0.02	1.68	1.06±0.03
$<\sigma_t^{-1}>$, δ^{-1}	0.381	0.380	0.413	0.412
$<\sigma_t^{-2}>$, δ^{-2}	0.168	0.168	0.194	0.194
$<\sigma_t^{-3}>$, δ^{-3}	0.085	0.085	0.103	0.102
$<\sigma_t^{-4}>$, δ^{-4}	0.048	0.048	0.060	0.059
$<\sigma_t^{-5}>$, δ^{-5}	0.029	0.029	0.037	0.036
σ_{tmin}	1.189	1.182±0.005	1.251	1.366±0.001
F_t	0.748	0.747±0.002	0.762	0.763
$(\sigma_{tmin})_\bullet$	1.189	1.183±0.006	1.251	1.26±0.08
$(\sigma_{tmax})_\bullet$	5.873	6.3±0.2	7.365	6.4±0.7

1 - Averaged $\sigma_t(E)$
2 - Analysis of T(y) model
3 - Averaged $\sigma_t(E)$
4 - Analysis of T(y) model

Table 2

Group constants for uranium

1	2	3	4
4.6 - 10 (12)	This paper	16.19±0.02	0.686±0.002
	[5]	16.4±0.3	0.68
	[7]	15.88	0.668
10 - 21 (11)	This paper	14.46±0.11	0.772±0.007
	[5]	14.5±0.2	0.76±0.002
	[7]	14.48	0.755
21 - 46 (10)	This paper	13.56±0.03	0.831±0.003
	[5]	13.5±0.2	0.83±0.02
	[7]	13.46	0.855
46 - 100 (9)	This paper	12.79±0.05	0.908±0.005
	[5]	12.71±0.10	0.914
	[7]	12.57	0.915

1 - Energy interval (No. of ABBN group)
2 - Reference
3 - $< \sigma_t >$, δ
4 - F_t

Table 3

Statistical characteristics of the energy dependence of the total neutron cross-sections for a natural mixture of chromium isotopes

<E>, keV (ΔE), keV	660 (150)		820 (140)	
$\langle\sigma_t\rangle$, δ	3.029±0.017	2.814	2.99±0.04	2.90
$D\sigma_t$, δ^2	3.11±0.20	2.02	1.60±0.07	1.65
$\langle\sigma_t^{-1}\rangle$, δ^{-1}	0.440	0.456	0.416	0.431
$\langle\sigma_t^{-2}\rangle$, δ^{-2}	0.256	0.279	0.219	0.236
$\langle\sigma_t^{-3}\rangle$, δ^{-3}	0.189	0.231	0.137	0.159
F_t	0.568	0.580	0.636	0.630
Origin	This paper	[8]	This paper	[8]

Table 4

Group constants for a natural mixture of chromium isotopes

Group number	Energy interval, MeV	$\langle\sigma_t\rangle$, barn			F_t		
		This paper	[9]	[10]	This paper	[9]	[10]
5	14 - 0.8	3.19	3.06	3.42	0.678	0.682	0.62
6	0.8 - 0.4	3.22	3.24	3.26	0.548	0.554	0.51

REFERENCES

[1] NIKOLAEV, M.N., FILIPPOV, V.V., At. Ehnerg. 15 (1963) 493 [in Russian].
[2] TARASKO, M.Z., The minimum directed divergence technique in problems involving the determination of distributions, Preprint FEhI-1446, Obninsk (1983) [in Russian].
[3] KOMAROV, A.V., LUK'YANOV, A.A., At. Ehnerg. 53 (1982) 392 [in Russian].
[4] VAN'KOV, A.A., UKRAINTSEV, V.F., YANEVA, N.B., et al., Analysis of Experimental Data on Neutron Transmission in the Unresolved Resonance Region for ^{239}Pu, Report P3-83-51, OIYaI [Joint Nuclear Research Institute], Dubna (1983) [in Russian].
[5] FILIPPOV, V.V., Vopr. At. Nauki i Tekhniki, Ser. Yad. Konstanty 4 (1985) 33 [in Russian].
[6] VAN'KOV, A.A., GOSTEVA, L.S., UKRAINTSEV, V.F., Vopr. At. Nauki i Tekhniki, Ser. Yad. Konstanty 3 (52) (1983) 27 [in Russian].
[7] ABAGYAN, L.P., BAZAZYANTS, N.O., NIKOLAEV, M.N., TSIBULYA, A.M., "Group Constants for Reactor and Shielding Calculations", Ehnergoizdat, Moscow, (1981) 231 [in Russian].
[8] OVDIENKO, V.D., SKLYAR, N.T., SMETANIN, G.A., et al., Neutron Physics, Vol. 3, TsNIIatominform, Moscow (1984) 84 [in Russian].
[9] VOZYAKOV, V.V., KOMAROV, A.V., KRIVTSOV, A.S., Neutron Physics, Vol. 3, TsNIIatominform, Moscow (1984) 107 [in Russian].
[10] FILIPPOV, V.V., Neutron Physics, Vol. 3, TsNIIatominform, Moscow (1984) 107 [in Russian].

Submitted for publication 14 July 1988